Stability of Ionic Liquids against Sodium Metal: A Comparative Study of 1-Ethyl-3-methylimidazolium Ionic Liquids with Bis(fluorosulfonyl)amide and Bis(trifluoromethylsulfonyl)amide

Takafumi Hosokawa[a], Kazuhiko Matsumoto[a, b], Toshiyuki Nohira[b,c]*, Rika Hagiwara[a,b], Atsushi Fukunaga[d], Shoichiro Sakai[d], Koji Nitta[d]*

[a]Graduate School of Energy Science, Kyoto University, Sakyo-ku, Kyoto 606–8501, Japan

[b]Unit of Elements Strategy Initiative for Catalysts & Batteries (ESICB), Kyoto University, Katsura, Kyoto 615-8510, Japan

[c]Institute of Advanced Energy, Kyoto University, Uji 611-0011, Japan

[d]Sumitomo Electric Industries Ltd., 1-1-3 Shimaya, Konohana-ku, Osaka 554-0024, Japan

Phone: +81 75 753 5827, Fax: +81 75 753 5906,

*E–mail: k-matsumoto@energy.kyoto-u.ac.jp (Kazuhiko Matsumoto) ; nohira.toshiyuki.8r@kyoto-u.ac.jp (Toshiyuki Nohira),

Abstract

The stability of $[C_2C_1im][FSA]$ ($C_2C_1im^+$: 1-ethyl-3-methylimidazolium and FSA^-: bis(fluorosulfonyl)amide) and $[C_2C_1im][TFSA]$ ($TFSA^-$: bis(trifluoromethylsulfonyl)amide) ionic liquids against Na metal has been investigated in view of their application as electrolytes for Na secondary batteries. Cyclic voltammetry revealed that Na metal electrodeposition/dissolution reactions occur in Na[FSA]–$[C_2C_1im][FSA]$, whereas these processes do not occur in Na[TFSA]–$[C_2C_1im][TFSA]$. Both visual and spectroscopic changes were observed for Na[TFSA]–$[C_2C_1im][TFSA]$ after immersion of Na metal for four weeks, but no changes were observed for Na[FSA]–$[C_2C_1im][FSA]$. X-ray photoelectron spectroscopy and electrochemical impedance spectroscopy indicated that there were differences in the thickness of the surface films on Na metal immersed in these ionic liquids. The presence of Na^+ also affects the thickness of the surface film, and the nature of the surface films determines the difference in the stability of Na metal in these two ionic liquids.

1 Introduction

Sodium secondary batteries are promising candidates for large-scale power storage devices, e.g., electric vehicles and renewable energy resources, owing to the abundance of Na resources and the high energy density arising from the low Na/Na^+ redox potential[1-5].

Although organic solutions, such as carbonates, are mostly used as electrolytes in Na secondary batteries[6-8], they are potentially dangerous due to the flammability and volatility of organic solvents. The unique properties of ionic liquids, such as nonflammability, negligible volatility, and high thermal and electrochemical stability, provide a solution to this issue[9,10]. In particular, FSA^- (bis(fluorosulfonyl)amide) and $TFSA^-$ (bis(trifluoromethylsulfonyl)amide) anion-based ionic liquids have reasonably high ionic conductivities and electrochemical stabilities. Consequently, many researchers have studied the properties of these ionic liquids for their application as electrolytes for Na secondary batteries[11-21].

Imidazolium-based ionic liquids have a high potential to improve the performance of ionic liquid electrolytes for Na secondary batteries because they have a higher ionic conductivity than quaternary ammonium and pyrrolidinium-based ionic liquids[19,22,23]. One of the main drawbacks of imidazolium-based ionic liquids is their poor stability against reduction, which is in contrast to those of quaternary ammonium-based ionic liquids. Because they reductively decompose at potentials more positive than the Li/Li^+ redox potential[24], their use as electrolytes for Li secondary batteries was believed to be difficult. However, two reports using FSA^--based ionic liquid electrolytes confirmed

stable Li^+ intercalation/deintercalation into graphite[25] and deposition/dissolution of Li metal[26] in the Li[TFSA]–[C_2C_1im][FSA] ionic liquid ($C_2C_1im^+$: 1-ethyl-3-methylimidazolium) without the use of any additives. This is in stark contrast to Li[TFSA]–[C_2C_1im][TFSA][25-28], which consists of only $TFSA^-$ anions, and shows differences in electrochemical behavior between [C_2C_1im][FSA]- and [C_2C_1im][TFSA]-based ionic liquids in negative potential regions.

For Na secondary batteries using ionic liquid electrolytes, the physicochemical properties of the Na[TFSA]–[C_2C_1im][TFSA] and Na[TFSA]–[C_4C_1im][TFSA] ($C_4C_1im^+$: 1-butyl-3-methylimidazolium) indicated that they were good electrolytes[29]. Although a reduction current for Na^+ was observed in Na[TFSA]–[C_4C_1im][TFSA], it overlapped with the reduction of the ionic liquid itself; consequently, reversible dissolution of Na metal was not observed[30]. In our previous report[31], Na[FSA]–[C_2C_1im][FSA] ionic liquids were shown to have good properties such as a wide liquid-phase temperature range, high ionic conductivity, and stable Na metal deposition/dissolution.

The stability of ionic liquids against Na metal is important for the use of a Na metal reference electrode in experimental works and its possible use as a negative electrode. However, thus far, there has been no systematic investigation on this topic. In this study, the stability of ionic liquid against Na metal was investigated for [C_2C_1im][FSA]- and [C_2C_1im][TFSA]-based ionic liquids for their use as electrolytes for Na secondary batteries. The electrodeposition/dissolution of Na metal in these ionic liquids was investigated by cyclic voltammetry. Changes in color of the ionic liquids before and after immersion of Na metal in these ionic liquids were confirmed by visual observation and

ultraviolet-visible (UV-VIS) spectroscopy. The surfaces of the immersed Na metal samples were analyzed by electrochemical impedance spectroscopy, optical microscopic observation, scanning electron microscopy, and X-ray photoelectron spectroscopy.

2 Experimental

Air sensitive materials were handled in a glovebox under a dried and deoxygenated argon atmosphere. The ionic liquids, $[C_2C_1im][FSA]$ (Kanto Chemical Co., Ltd.) and $[C_2C_1im][TFSA]$ (Ionic Liquids Technologies GmbH) were purchased and dried under vacuum at 363 K for 24 h (water content < 10 ppm for both). The Na salts, Na[FSA] (Mitsubishi Materials Electronic Chemicals Co., Ltd.) and Na[TFSA] (Morita Chemical Industries Co., Ltd.) were dried under vacuum at 363 K for more than 24 h (water content < 40 ppm). Water content was measured by Karl-Fischer titration (Metrohm, 899 Coulometer).

Cyclic voltammetry was performed in a three-electrode cell at 298 K in a glovebox using an electrochemical measurement system (Biologic, VSP-300) at a scan rate of 5 mV s^{-1}. A Cu disk (diameter, 1.6 mm) and a Na plate were used as working and counter electrodes, respectively. A reference electrode was made of a Ag wire immersed in $[C_2C_1im][FSA]$ or $[C_2C_1im][TFSA]$ containing 0.05 mol kg^{-1} $Ag[SO_3CF_3]$ separated from the electrolyte by porous glass.

The stability of Na metal was tested against seven types of ionic liquids, as summarized in Table 1 (A: neat $[C_2C_1im][FSA]$, B: neat $[C_2C_1im][TFSA]$, C: Na[FSA]−$[C_2C_1im][FSA]$ (10:90 in molar ratio), D:

Na[TFSA]−[C_2C_1im][TFSA] (10:90), E: Na[TFSA]−[C_2C_1im][FSA] (10:90), F: Na[FSA]−[C_2C_1im][TFSA] (10:90), and G: Na[FSA]−[C_2C_1im][TFSA] (1:99)). A slice of Na metal (approximately 5 × 5 × 0.2 mm) was immersed in each ionic liquid for four weeks. The UV-VIS spectra were measured by a UV-VIS spectrometer (Hitachi, U-3010).

For electrochemical impedance spectroscopy, two-electrode cells (2032 coin cell) were assembled in the glovebox. Both the working and counter electrodes were Na metal. The electrochemical impedance spectra (EIS) were recorded by an electrochemical measurement system (Biologic, VSP-300) at room temperature. Frequency ranged from 20 kHz to 10 mHz with an AC amplitude of 20 mV.

Visual changes in the Na metal surface after immersion in the ionic liquids for one week were observed by a digital microscope (Keyence, VHX-5000). The samples were placed in an air-tight chamber with a quartz window without rinsing the ionic liquids from the metal. The surface morphologies of Na metal immersed in ionic liquids for one week were also observed using field-emission scanning electron microscope (FE-SEM, Hitachi SU-8020). Samples were prepared for FE-SEM observation both with and without rinsing with tetrahydrofuran (THF, water content < 10 ppm, oxygen content < 1 ppm; Wako Pure Chemical Industries, Ltd.) to remove the ionic liquids.

A solid reaction product obtained after immersion of Na metal in Na[TFSA]–[C_2C_1im][TFSA] for over one year was analyzed by X-ray diffraction (XRD) using a SmartLab diffractometer (Rigaku; Cu-Kα radiation, λ = 0.15418 nm) equipped with a one-dimensional, high-speed detector (D/teX Ultra, Rigaku). The measurement was performed at 40 kV and 30 mA. The sample was washed with THF prior

to analysis and placed in an air-tight cell with a beryllium window under a dry argon atmosphere.

The surface composition was analyzed by X-ray photoelectron spectroscopy (JEOL, JPS-9010) with Al *K*α radiation. The samples were washed with THF prior to analysis to remove residual ionic liquids on the metal surface and were introduced into the analyzing chamber with an air-tight transfer vessel without air exposure. Depth profiles were obtained by argon ion etching for 5, 15, 30, 60, and 90 s.

3 Results and discussion

3.1 Na metal electrodeposition/dissolution in FSA^- and $TFSA^-$-based ionic liquids

Figure 1(a) shows cyclic voltammograms of a Cu disk electrode in $[C_2C_1im][FSA]$ and $Na[FSA]–[C_2C_1im][FSA]$ (10:90 in molar ratio). A cathodic current corresponding to the decomposition of the ionic liquid was observed at around −2.9 V vs. Ag/Ag^+ in $[C_2C_1im][FSA]$. This cathodic current is mainly ascribed to the reduction of $C_2C_1im^+$, considering the electrochemical behavior of $C_2C_1im^+$-based ionic liquids with cathodically stable anions[32]. A small anodic current around −1.3 V vs. Ag/Ag^+ is assigned to the oxidation of the product formed during the adjacent cathodic scan. A pair of cathodic and anodic currents was observed around −3.4 V vs. Ag/Ag^+ in $Na[FSA]–[C_2C_1im][FSA]$. These results indicate that stable electrodeposition/dissolution of Na metal occurs in $Na[FSA]–[C_2C_1im][FSA]$, as we have previously demonstrated for $Na[FSA]–[C_2C_1im][FSA]$ (30:70)[31]. Figure 1(b) shows cyclic voltammograms of Cu disk electrodes in $[C_2C_1im][TFSA]$ and $Na[TFSA]–[C_2C_1im][TFSA]$ (10:90 in molar ratio). The voltammogram for $[C_2C_1im][TFSA]$ is quite similar to that of $[C_2C_1im][FSA]$. In the

case of Na[TFSA]–[C_2C_1im][TFSA], the cathodic limit is extended to around −3.5 V vs. Ag/Ag^+, which is again similar to that of the Na[FSA]–[C_2C_1im][FSA] system; however, the anodic current corresponding to dissolution of Na metal is missing. The small cathodic current in the range between −2.5 and −3.5 V vs. Ag/Ag^+ is attributed to the decomposition of the ionic liquid, although the current is significantly suppressed compared to that of neat [C_2C_1im][TFSA]. Similar behavior has been reported for the Li[TFSA]–[C_2C_1im][FSA] system[26]. We could not confirm whether the cathodic current at around −3.5 V corresponds to deposition of Na metal; even if so, deposited Na metal may react with the $TFSA^-$-based ionic liquid immediately after the deposition, as described later.

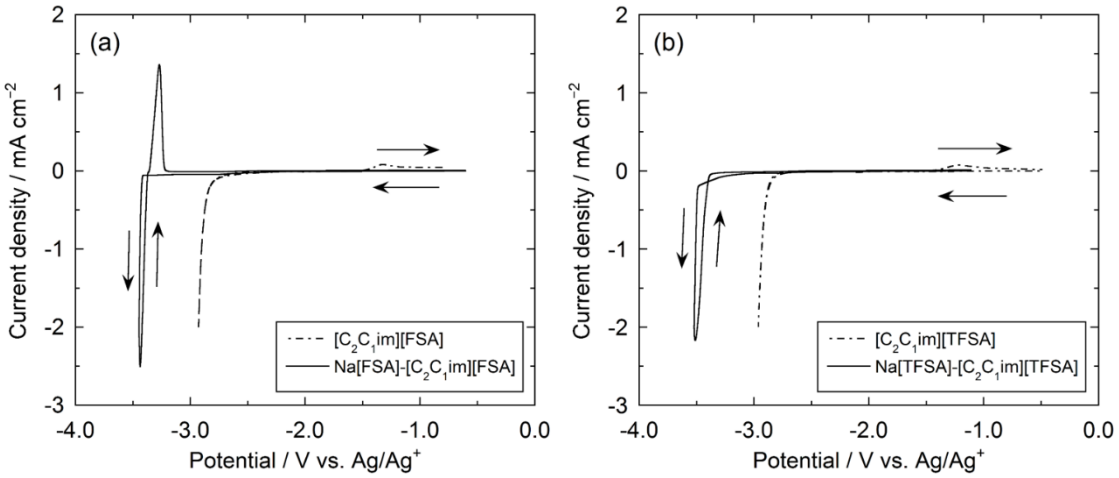

Figure 1 Cyclic voltammograms of a Cu disk electrode in (a) [C_2C_1im][FSA] and Na[FSA]–[C_2C_1im][FSA] (10:90) and (b) [C_2C_1im][TFSA] and Na[TFSA]–[C_2C_1im][TFSA] (10:90) at 298 K. Scan rate: 5 mV s^{-1}.

The potential for reductive decomposition of $C_2C_1im^+$ is more positive than the Na/Na^+ redox potential, as shown in Figure 1(a). Thus, the presence of Na^+ in FSA^--based ionic liquids prevents decomposition of $C_2C_1im^+$ at the electrode and enables stable deposition/dissolution of Na metal,

underscoring the advantage of using FSA^--based ionic liquids as electrolytes for Na secondary batteries. However, the results for FSA^-- and $TFSA^-$-based ionic liquids differ from those previously reported for other cations. For example, in both the pyrrolidinium FSA- and TFSA ionic liquids, the deposition/dissolution of Na was observed[14,20,30,33]. Therefore, both anionic species and cationic species determine the cathode limit of the ionic liquids. According to previous investigation on Li[TFSA]−[C_2C_1im][FSA][34], the extension of the cathode limit and stable intercalation/deintercalation of Li^+ into/from graphite in FSA^--based ionic liquids have been explained by changes to the structure of the electric double-layer. However, the observed cathode behavior in the present study cannot be explained simply by the cyclic voltammetry measurements.

3.2 Reactivity of FSA^- and $TFSA^-$-based ionic liquids with Na metal

Table 1 summarizes the changes in appearance and UV-VIS spectra of the ionic liquids (A to G) after immersion of Na metal for four weeks. All the ionic liquids were colorless and transparent before immersion of the Na metal (Figure 2). After the immersion, samples B (pure [C_2C_1im][TFSA]) and D (Na[TFSA]:[C_2C_1im][TFSA] = 10:90) became brown. In sample B, the Na sample floated on initial placement into the sample, but after four weeks, sank into the ionic liquid. Furthermore, the sodium became smaller and became transparent after several months immersed in the ionic liquid (Na immersed in D also showed similar change after several months, and these changes were examined by XRD measurement, as mentioned below). These results indicate that Na metal reacts with the pure

[C_2C_1im][TFSA] ionic liquid, and the reaction product has a greater density than that of the ionic liquid. Sample G (Na[FSA]:[C_2C_1im][TFSA] = 1:99) changed color slightly. Color changes for B, D, and G were also measured by UV-VIS spectroscopy between 250 and 600 nm, as shown in Figure 3. Although there was no change in appearance for A ([C_2C_1im][FSA]), the spectrum of A changed after Na immersion at around 290 nm. In contrast, samples C (Na[FSA]:[C_2C_1im][FSA] = 10:90), E (Na[TFSA]:[C_2C_1im][FSA] = 10:90) and F (Na[FSA]:[C_2C_1im][TFSA] = 10:90) showed no changes after Na metal immersion, based on both appearance and UV-VIS spectra.

Table 1 Summary of Na metal immersion tests by visual confirmation and UV-VIS spectroscopy for seven ionic liquids.

	A	B	C	D	E	F	G
Na^+	–	–	FSA^- 10%	$TFSA^-$ 10%	$TFSA^-$ 10%	FSA^- 10%	FSA^- 1%
$C_2C_1im^+$	FSA^- 100%	$TFSA^-$ 100%	FSA^- 90%	$TFSA^-$ 90%	FSA^- 90%	$TFSA^-$ 90%	$TFSA^-$ 99%
Color change	N. C.[a]	Intense	N. C.	Intense	N. C.	N. C.	Weak
Change in UV-VIS	Slight	Large	N. C.	Large	N. C.	N. C.	Slight

[a] N. C.: No change.

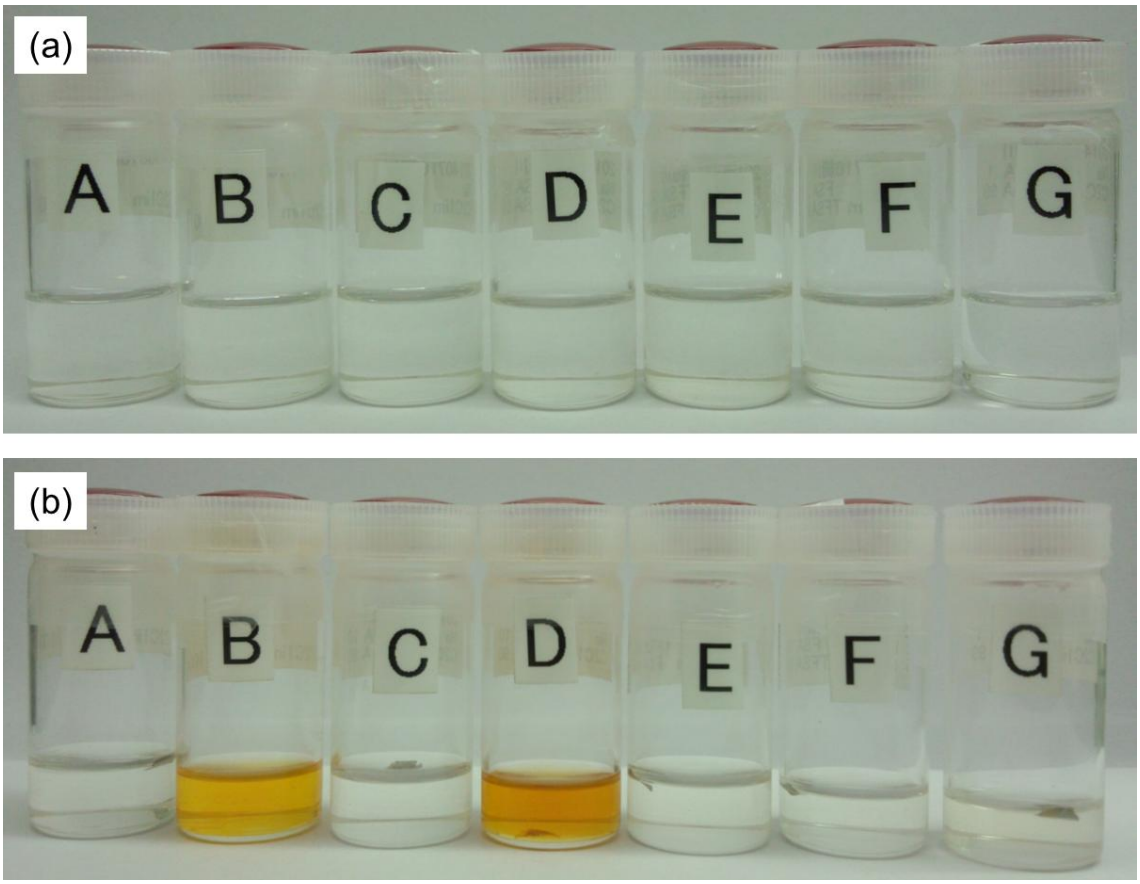

Figure 2 Photographs of the seven ionic liquids (a) before Na metal immersion and (b) after Na metal immersion for four weeks. The symbols correspond to the ionic liquids shown in Table 1.

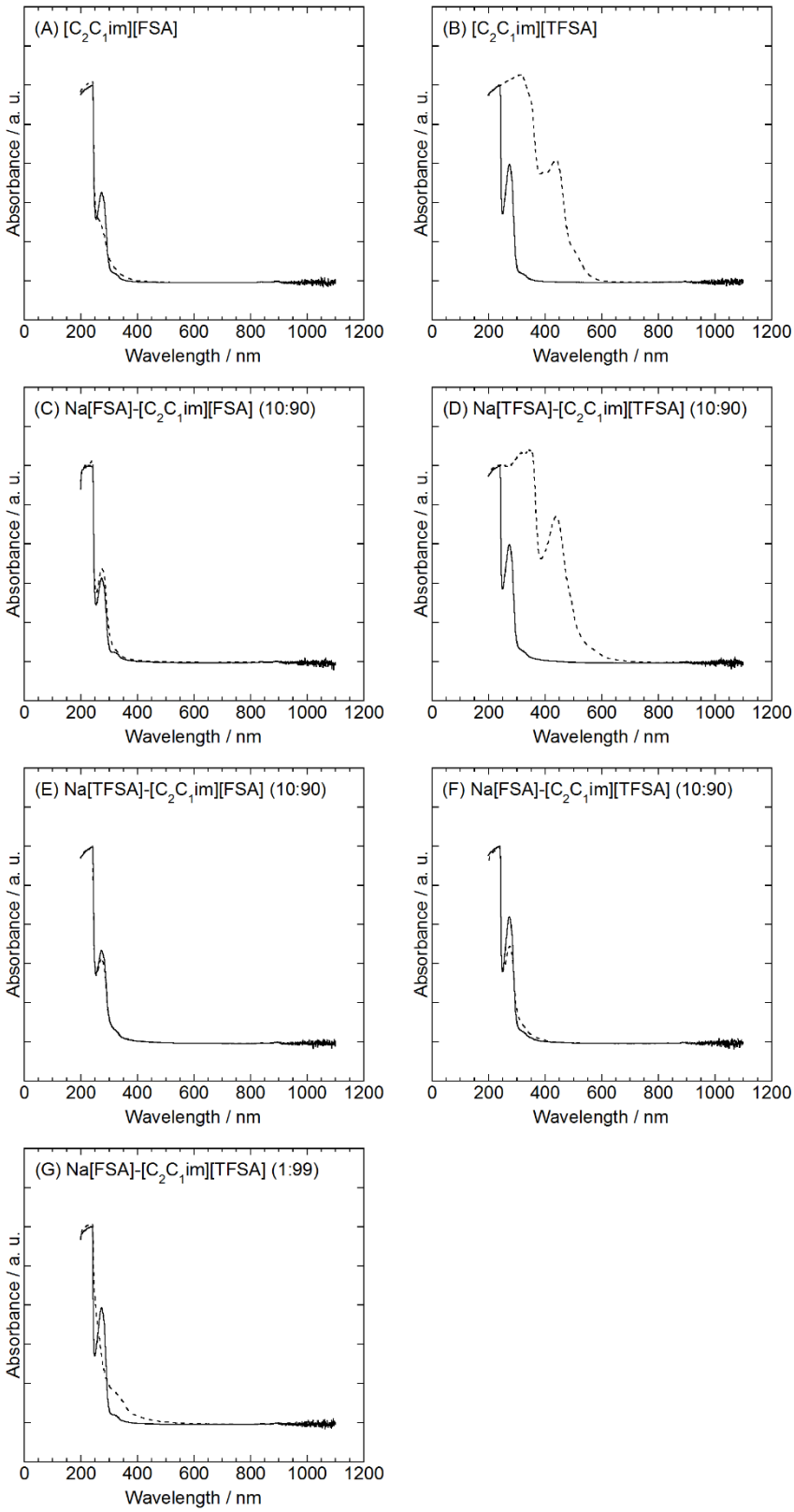

Figure 3 Ultraviolet-visible spectra for the seven ionic liquids before (solid line) and after (dotted line) immersion of sodium metal for four weeks.

These results indicate that $[C_2C_1im][TFSA]$ is not stable with Na metal, regardless of the presence of Na^+ cations. The chemical reaction between Na metal and the ionic liquids is suppressed even in the presence of 1 mol% FSA^- of total anion content, and the presence of 10% of FSA^- is also quite effective. Although samples A and C contained no $TFSA^-$, there was a little difference in their behavior; the color of A changed slightly, but that of C did not. The difference suggests that Na^+ also plays an important role to improve the stability of the ionic liquids against Na metal even if FSA^- is only the component anion.

Additionally, NMR measurements of the ionic liquids after Na metal immersion were performed to detect the decomposition products. Unfortunately, the changes in the spectrum were too small to identify the decomposition products.

3.3 The change of electrochemical impedance spectra with time for Na/ionic liquid/Na symmetric cells

Figures 4(a) and (b) show the EIS spectra of Na/ionic liquid/Na symmetric cells one hour and one week after assembly, respectively, for $[C_2C_1im][FSA]$, $[C_2C_1im][TFSA]$, Na[FSA]–$[C_2C_1im][FSA]$ (10:90), and Na[TFSA]–$[C_2C_1im][TFSA]$ (10:90). Because Na^+ ions are not present in either $[C_2C_1im][FSA]$ and $[C_2C_1im][TFSA]$, the open circuit potential of Na electrode may have shifted during the impedance measurements in these pure ionic liquids. Nevertheless, the possible potential shift was considered small due to the immediate formation of a surface film containing Na^+. For all the ionic

liquids, the semicircles obtained in the EIS plots after one week were enlarged, suggesting that reaction of Na metal with ionic liquids occurred. However, significant increases in the size of the semicircles in the EIS spectra were observed for the $TFSA^-$-based ionic liquids, suggesting the formation of a resistive film. The increase of resistance for Na[FSA]−[C_2C_1im][FSA] was smaller than that for neat [C_2C_1im][FSA]. Figures 4(c) and (d) shows the time dependence of EIS spectra for [C_2C_1im][FSA] and Na[FSA]–[C_2C_1im][FSA] (10:90) (10 minutes, 6 hours, 1 day, 1 week, and 2 weeks after assembly), respectively. For [C_2C_1im][FSA], the semicircles gradually became larger as the immersion time increased. Although the same behavior was also observed for Na[FSA]–[C_2C_1im][FSA], the rate of increase was small in this case. Moreover, the EIS spectrum obtained at two weeks overlaps that obtained after one week, suggesting that the reaction between Na metal and the electrolyte had ceased. These observations suggest that Na metal reacts both with [C_2C_1im][FSA] and Na[FSA]–[C_2C_1im][FSA], but the reaction with the latter is significantly suppressed by the formation of a protective film. The EIS results are consistent with the differences in color changes after immersion of Na metal in the samples, as mentioned above.

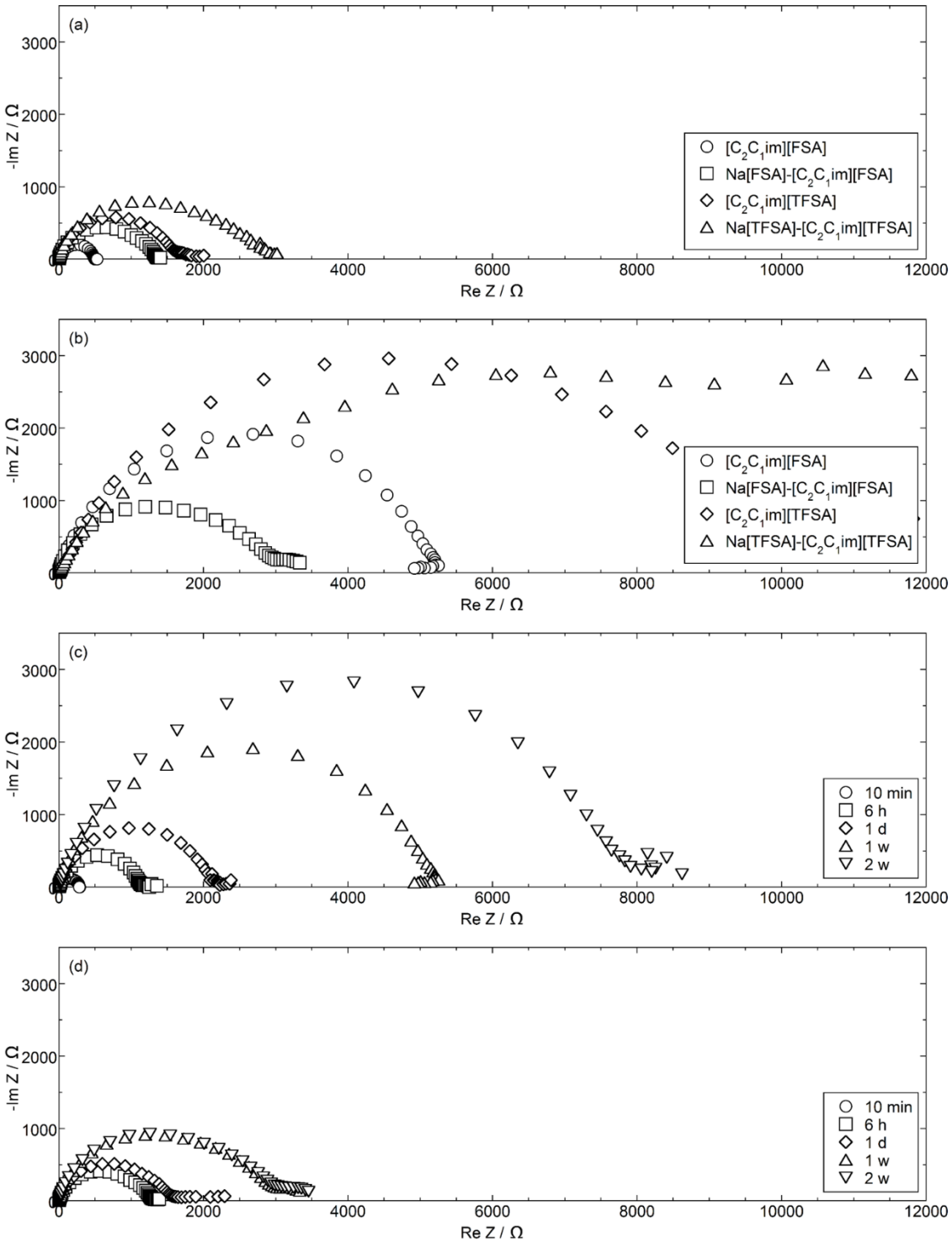

Figure 4 Electrochemical impedance spectra of the Na/ionic liquid/Na symmetric cells: Spectra (a) at 1 hour and (b) 1 week after assembly for $[C_2C_1im][FSA]$, $[C_2C_1im][TFSA]$, Na[FSA]–$[C_2C_1im][FSA]$ (10:90), and Na[TFSA]–$[C_2C_1im][TFSA]$ (10:90). Time dependence of spectra for (c) $[C_2C_1im][FSA]$ and (d) Na[FSA]–$[C_2C_1im][FSA]$ (10 minutes, 6 hours, 1 day, 1 week, and 2 weeks).

3.4 Analysis of the Na metal surface immersed in ionic liquids

Figure 5 shows optical microscopic images of the Na metal surface before and after immersion in Na[FSA]–[C_2C_1im][FSA] (10:90) and Na[TFSA]–[C_2C_1im][TFSA] (10:90) for one week. Distinct differences are observed between the surfaces immersed in the FSA^-- and $TFSA^-$-based ionic liquids (Figure 5(a)). The surface of pristine Na metal (Figure 5(b), observed with different angles of illumination because of metallic luster) was smooth except for visible lines caused by cutting. In contrast, the surface immersed in Na[FSA]–[C_2C_1im][FSA] (Figure 5(c)) was covered with a thin layer and different from the pristine sample; however, it retained its metallic luster. On the other hand, the surface immersed in Na[TFSA]–[C_2C_1im][TFSA] (Figure 5(d)) became dark in color and rough in texture.

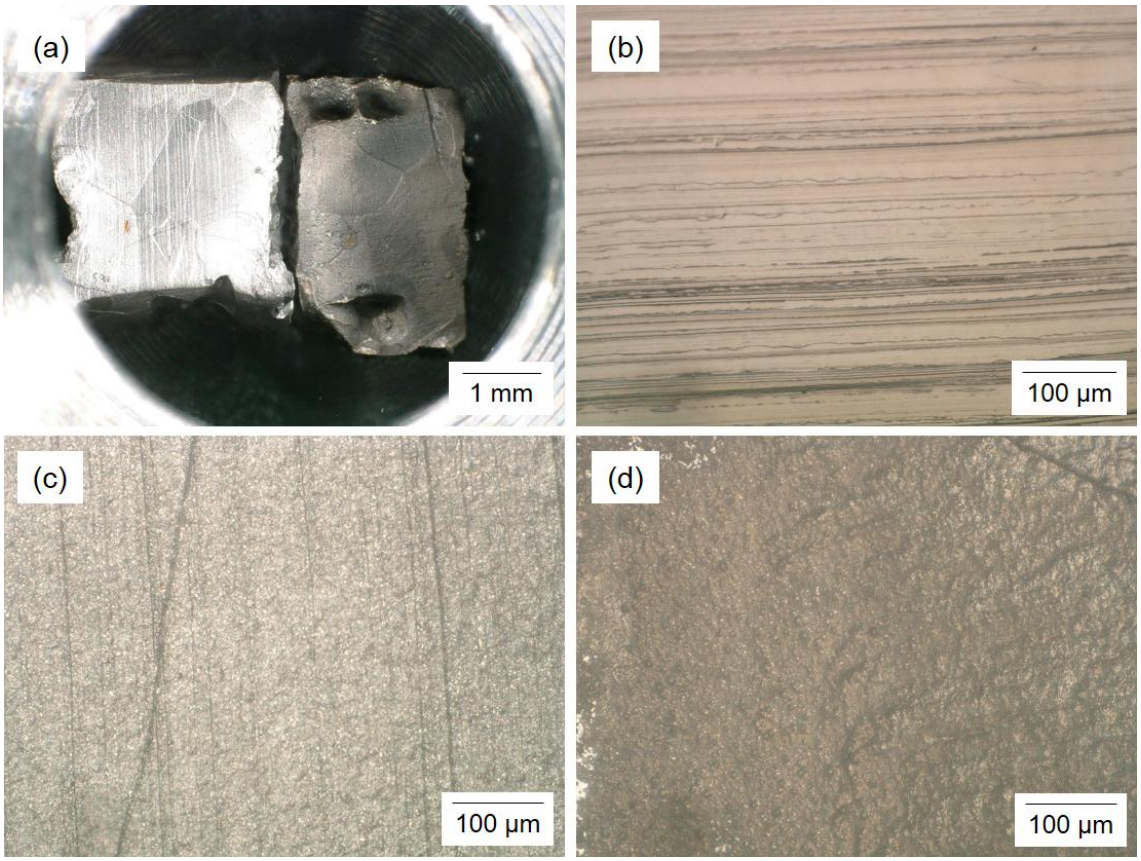

Figure 5 Optical microscopic images of Na metal surface immersed in (a) Na[FSA]–[C_2C_1im][FSA] (10:90) (left) and Na[TFSA]–[C_2C_1im][TFSA] (10:90) (right) for one week at low magnification, (b) before immersion, (c) immersed in Na[FSA]–[C_2C_1im][FSA] (10:90) for one week, and (d) immersed in

Na[TFSA]–[C_2C_1im][TFSA] (10:90) for one week.

Figure 6 shows an XRD pattern of a solid reaction product obtained by immersing Na metal in Na[TFSA]–[C_2C_1im][TFSA] over a period of one year, as mentioned in Section 3.2. The observed diffraction peaks were assigned to those of NaF, although they are weak and broad. Thus, it is suggested that one decomposition product of Na metal in contact with $TFSA^-$-based ionic liquids is NaF.

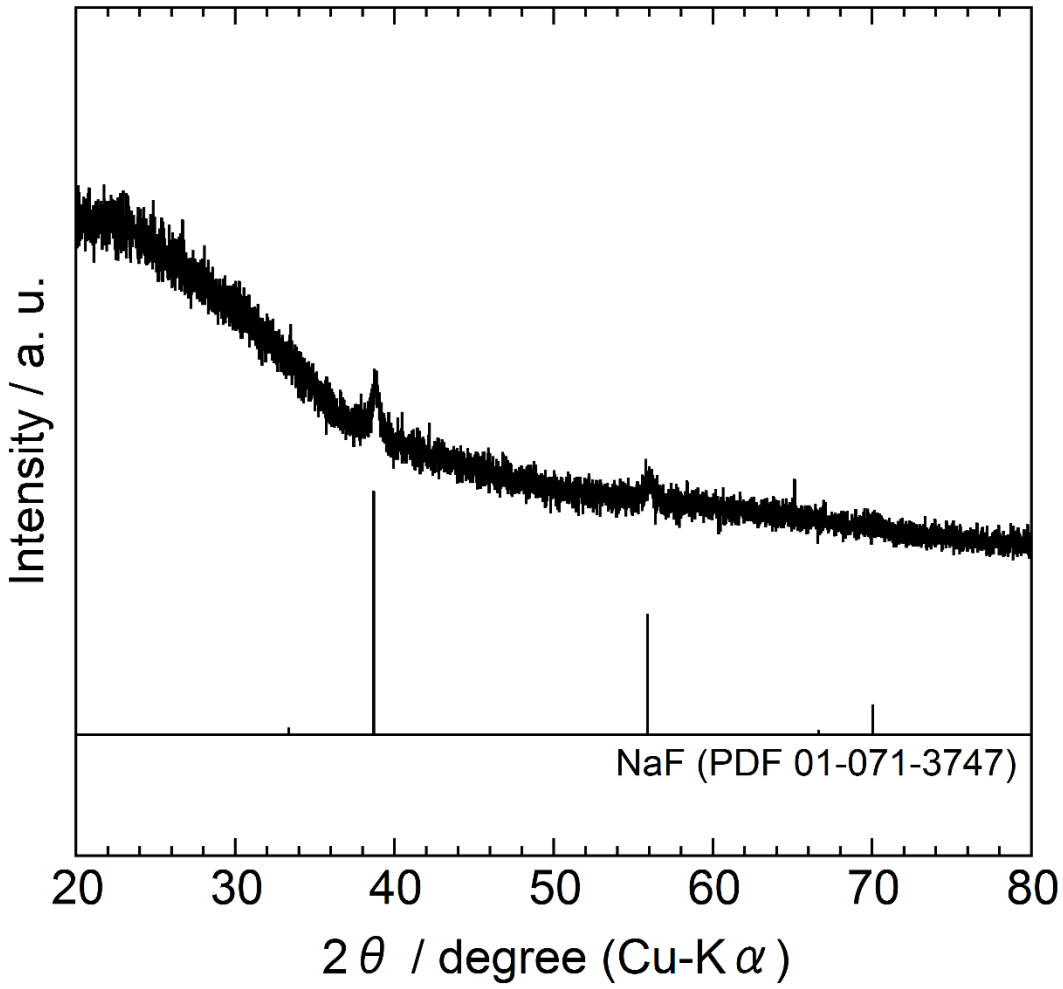

Figure 6 An X-ray diffraction pattern of a solid reaction product obtained by immersing Na metal in Na[TFSA]–[C_2C_1im][TFSA] over one year.

Figure 7 shows the XPS spectra over a wide range of binding energies for the Na metal surface before and after immersion in $[C_2C_1im][FSA]$, $[C_2C_1im][TFSA]$, Na[FSA]–$[C_2C_1im][FSA]$ (10:90), and Na[TFSA]–$[C_2C_1im][TFSA]$ (10:90) for one week (etching time: 5 s). Although peaks corresponding to elements arising from the anion (N, F, S, and O) were observed, the F1s peak was the most distinct, indicating the decomposition of FSA^- or $TFSA^-$ anions. The intensities of the F1s peak are weak for the FSA^--based ionic liquids compared with those for the $TFSA^-$-based ionic liquids. Thus, the F1s peak was used to investigate the properties of the surface films, as discussed next.

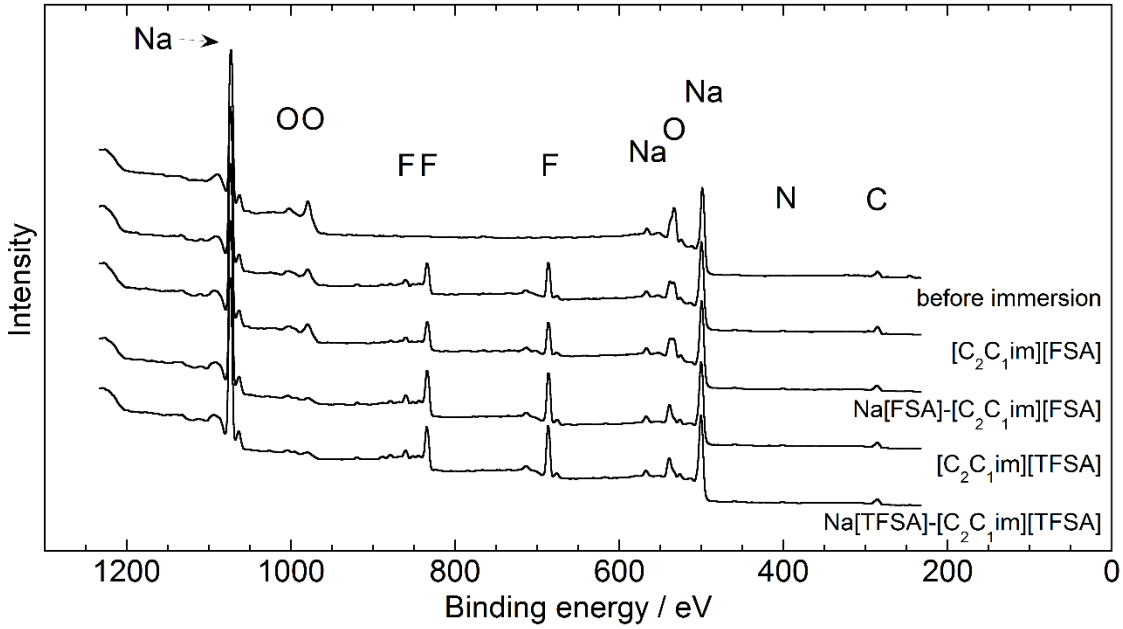

Figure 7 X-ray photoelectron spectra of Na metal before and after immersion in $[C_2C_1im][FSA]$, Na[FSA]–$[C_2C_1im][FSA]$ (10:90), $[C_2C_1im][TFSA]$, and Na[TFSA]–$[C_2C_1im][TFSA]$ (10:90) for one week. Etching time: 5 s.

Figure 8 shows the changes of F1s XPS spectra with Ar ion etching time for the Na metal surfaces immersed in the four ionic liquids. For reference, C1s, N1s, O1s, Na1s, and S2p XPS spectra are shown in Figures S1–S5 (Supporting Information). As the etching time increased, the F1s peak intensity

became smaller, indicating that the Na metals were covered by thin films containing fluorine atoms. However, the decrease in peak intensity was remarkably slow for the Na metal immersed in Na[TFSA]–[C_2C_1im][TFSA], indicating the presence of a thicker film.

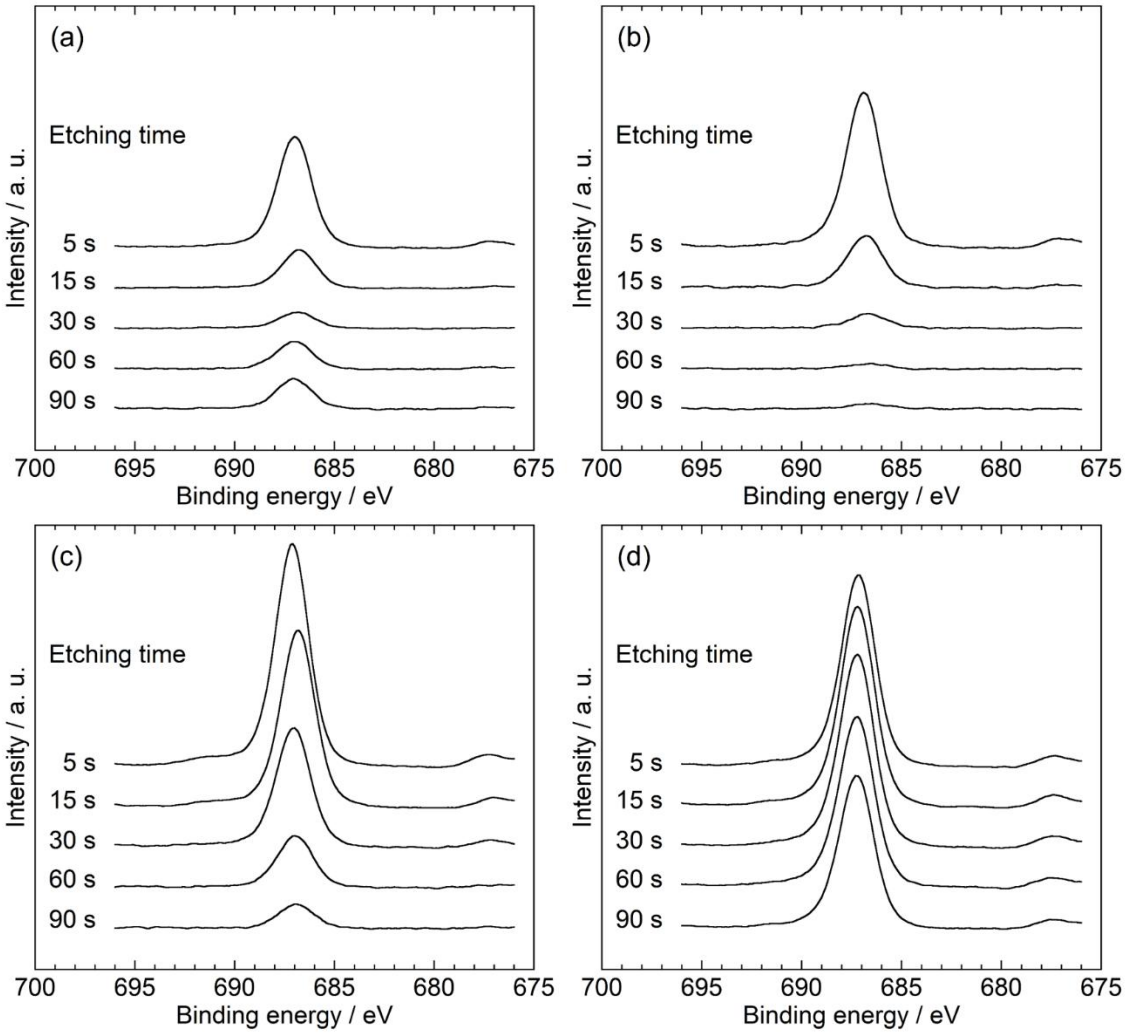

Figure 8 F1s X-ray photoelectron spectra of Na metal after immersion in (a) [C_2C_1im][FSA], (b) Na[FSA]–[C_2C_1im][FSA] (10:90), (c) [C_2C_1im][TFSA], and (d) Na[TFSA]–[C_2C_1im][TFSA] (10:90) for one week. Etching time: 5–90 s.

As shown in Figure 9, the change in the F/Na ratio with etching time was calculated from the XPS data. For the Na metal immersed in Na[TFSA]–[C_2C_1im][TFSA], the F/Na ratio gently decreased as etching time increased, implying formation of a thick film on the surface of Na metal immersed in

Na[TFSA]–[C_2C_1im][TFSA]. In contrast, the Na metals in FSA^--based ionic liquids had much thinner films; however, the F/Na ratio was low in the case of Na[FSA]–[C_2C_1im][FSA] compared with that of neat [C_2C_1im][FSA] over the whole etching period. These observations, based on XPS, agree with the results of EIS. In addition, the film on the Na metal immersed in [C_2C_1im][TFSA] is thinner than that immersed in Na[TFSA]–[C_2C_1im][TFSA], as calculated from the smaller F/Na ratio.

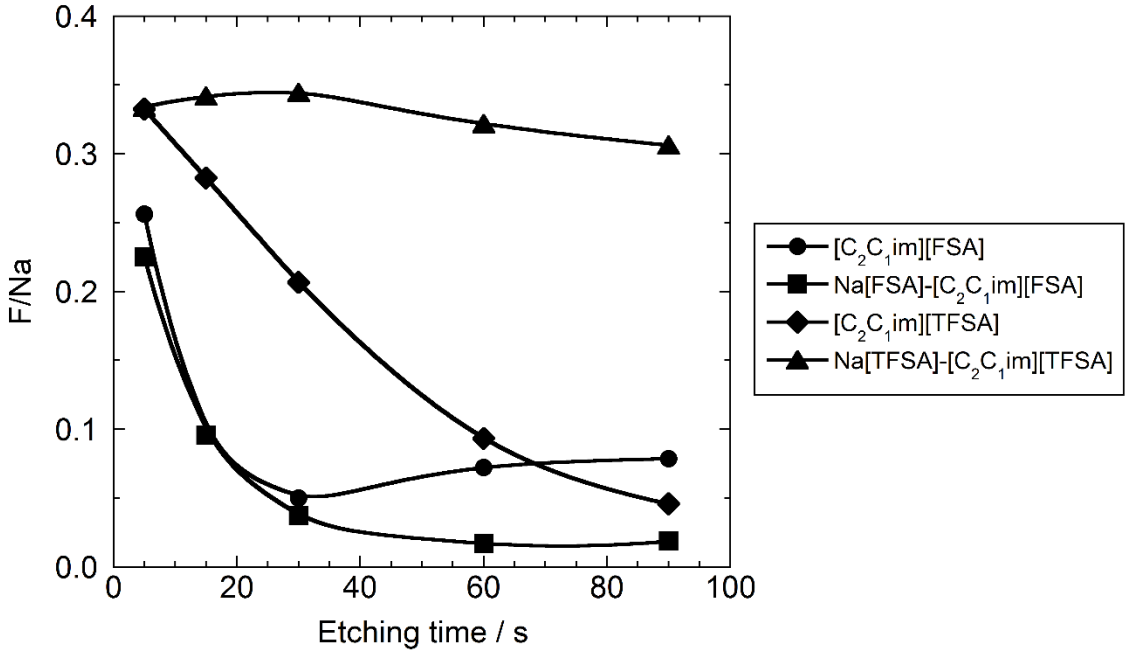

Figure 9 The F/Na ratio of Na metal surface immersed in ionic liquids ([C_2C_1im][FSA], Na[FSA]–[C_2C_1im][FSA] (10:90), [C_2C_1im][TFSA], and Na[TFSA]–[C_2C_1im][TFSA] (10:90)) obtained from XPS measurements as a function of etching time.

Although both these ionic liquids reacted chemically with Na metal and surface films formed, their stabilities are not the same. According to XPS results, the chemical compositions of the surface films for FSA^--based and $TFSA^-$-based ionic liquids do not significantly differ. A recent paper suggested that FSA^- reductively produces a radical anion and its unusually low reactivity facilitates the formation of stable surface film[35]. This is not the case for the $TFSA^-$-based salts, which is also confirmed in the

present study by the continuous growth of the surface film on Na metal in TFSA-based ionic liquids over time (see EIS and XPS results above). By considering these observations, both FSA- and TFSA ionic liquids reductively decompose in the presence of Na metal but the difference in reaction path and property of the surface film is considered to result in the higher stability of FSA^--based ionic liquids than the $TFSA^-$-based ionic liquids. This is possibly analogous to the Li system[36,37].

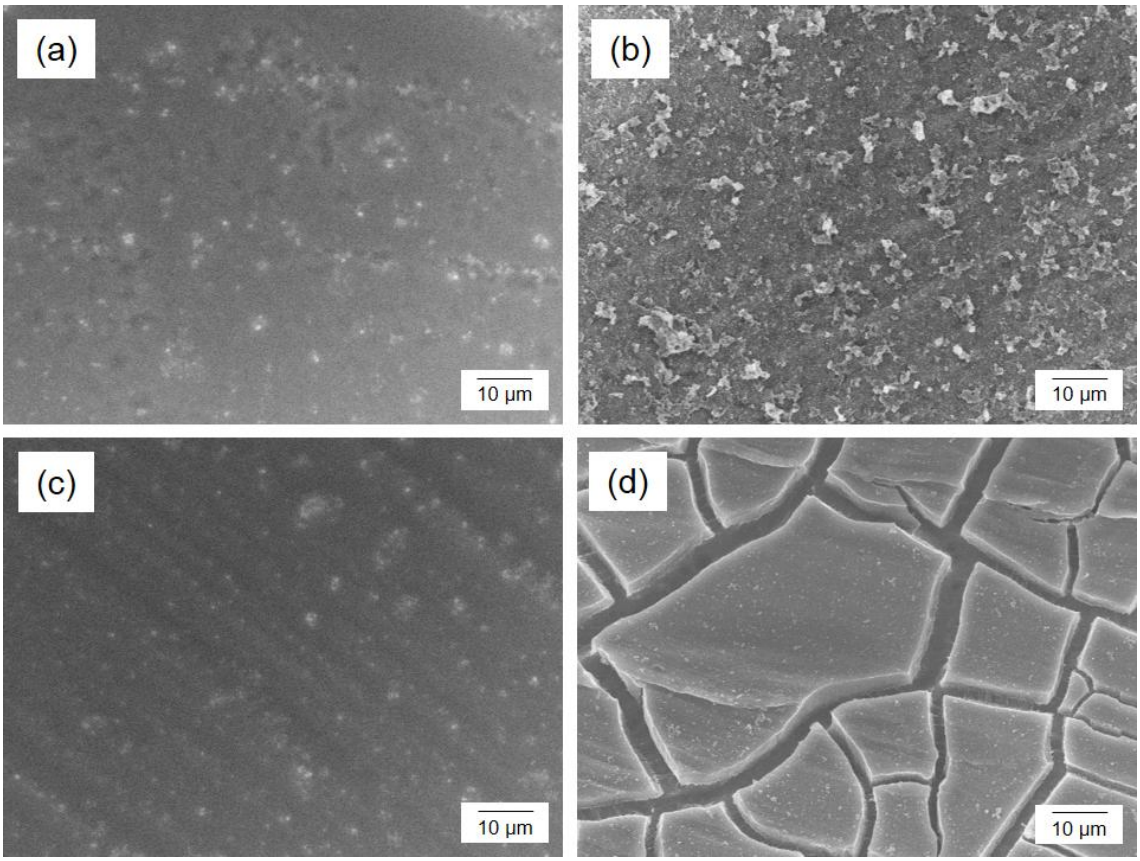

Figure 10 Scanning electron microscopic images of the surface of Na metal immersed in Na[FSA]–[C_2C_1im][FSA] (a) before and (b) after rinsing with THF and in Na[TFSA]–[C_2C_1im][TFSA] (c) before and (d) after rinsing with THF.

Another possible reason for the difference in stability against Na metal is the permeability of the ionic

liquids through the film, which may be supported by surface SEM observations in Figure 10. The Na metal surface immersed in the $TFSA^-$-based ionic liquid cracked after washing with THF, which was not observed for the one in the FSA^--based ionic liquid. Although this may arise from the amount of the absorbed ionic liquid in the surface, quantitative discussion is difficult because of the lack of the information on the film thickness.

4 Conclusion

Based on cyclic voltammetry measurements, Na metal deposition/dissolution was confirmed in Na[FSA]–[C_2C_1im][FSA] but not in Na[TFSA]–[C_2C_1im][TFSA]. The stability of Na metal against [C_2C_1im][FSA] and [C_2C_1im][TFSA] was investigated both in the presence or absence of the corresponding Na salts. After immersion of Na metal in the ionic liquids, both the ionic liquids and the surface of the Na metal sample were analyzed, which indicated that the presence of FSA^- dramatically improves the stability of the ionic liquids against Na metal. The contribution of Na^+ to the high stability against Na metal was also confirmed. Such behavior is related to the stability of formation of a surface film due to interaction of Na metal and the ionic liquids. These results suggest favor the use of FSA^--based ionic liquids as electrolytes for Na secondary batteries.

Acknowledgements

A part of this work was performed under a management of ‘Elements Strategy Initiative for Catalysts

& Batteries (ESICB)' supported by Ministry of Education, Culture, Sports, Science, and Technology, Japan (MEXT).

References

(1) Pan, H. L.; Hu, Y. S.; Chen, L. Q. Room-Temperature Stationary Sodium-Ion Batteries for Large-Scale Electric Energy Storage. *Energy Environ. Sci.* **2013,** *6*, 2338-2360.

(2) Ellis, B. L.; Nazar, L. F. Sodium and Sodium-ion Energy Storage Batteries. *Solid State Mater. Sci.* **2012**, *16*, 168-177.

(3) Kim, S. W.; Seo, D. H.; Ma, X; Ceder, G.; Kang, K. Electrode Materials for Rechargeable Sodium-Ion Batteries: Potential Alternatives to Current Lithium-Ion Batteries. *Adv. Energy. Mater.* **2012**, *2*, 710-721.

(4) Ponrouch, A.; Monti, D.; Boschin, A.; Steen, B.; Johansson, P.; Palacin, M. R. Non-aqueous Electrolytes for Sodium-ion Batteries. *J. Mater. Chem. A* **2015**, *3*, 22-42.

(5) Kundu, D.; Talaie, E.; Duffort, V.; Nazar, L. F. The Emerging Chemistry of Sodium Ion Batteries for Electrochemical Energy Storage. *Angew. Chem. Int. Ed.* **2015**, *54*, 3431-3448.

(6) Kuratani, K.; Uemura, N.; Senoh, H.; Takeshita, H. T.; Kiyobayashi, T. Conductivity, Viscosity and Density of $MClO_4$ (M = Li and Na) Dissolved in Propylene Carbonate and γ-Butyrolactone at High Concentrations. *J. Power Sources* **2013**, *223*, 175-182.

(7) Hong, S. Y.; Kim, Y.; Park, Y.; Choi, A.; Choi, N. S.; Lee, K. T. Charge Carriers in Rechargeable Batteries: Na Ions vs. Li Ions. *Energy Environ. Sci.* **2013**, *6*, 2067-2081.

(8) Ponrouch, A.; Dedryvere, R.; Monti, D.; Demet, A. E.; Mba, J. M. A.; Croguennec, L.; Masquelier, C.; Johansson, P.; Palacin, M. R. Towards High Energy Density Sodium Ion Batteries through

Electrolyte Optimization. *Energy Environ. Sci.* **2013,** *6*, 2361-2369.

(9) Ohno, H., *Electrochemical Aspects of Ionic Liquids*. 2nd ed.; John Wiley & Sons Inc.: Hoboken, New Jersey, 2011.

(10) MacFarlane, D. R.; Tachikawa, N.; Forsyth, M.; Pringle, J. M.; Howlett, P. C.; Elliott, G. D.; Davis, J. H.; Watanabe, M.; Simon, P.; Angell, C. A. Energy Applications of Ionic Liquids. *Energy Environ. Sci.* **2014,** *7*, 232-250.

(11) Kubota, K.; Nohira, T.; Hagiwara, R. New Inorganic Ionic Liquids Possessing Low Melting Temperatures and Wide Electrochemical Windows: Ternary Mixtures of Alkali Bis(fluorosulfonyl)amides. *Electrochim. Acta* **2012**, *66*, 320-324.

(12) Nohira, T.; Ishibashi, T.; Hagiwara, R. Properties of an Intermediate Temperature Ionic Liquid NaTFSA–CsTFSA and Charge–discharge Properties of $NaCrO_2$ Positive Electrode at 423 K for a Sodium Secondary Battery. *J. Power Sources* **2012**, *205*, 506-509.

(13) Fukunaga, A.; Nohira, T.; Kozawa, Y.; Hagiwara, R.; Sakai, S.; Nitta, K.; Inazawa, S. Intermediate-Temperature Ionic Liquid NaFSA-KFSA and Its Application to Sodium Secondary Batteries. *J. Power Sources* **2012,** *209*, 52-56.

(14) Noor, S. A. M.; Howlett, P. C.; MacFarlane, D. R.; Forsyth, M. Properties of Sodium-Based Ionic Liquid Electrolytes for Sodium Secondary Battery Applications. *Electrochim. Acta* **2013,** *114*, 766-771.

(15) Moreno, J. S.; Maresca, G.; Panero, S.; Scrosati, B.; Appetecchi, G. B. Sodium-conducting Ionic

Liquid-based Electrolytes. *Electrochem. Commun.* **2014**, *43*, 1-4.

(16) Wongittharom, N.; Wang, C.-H.; Wang, Y.-C.; Yang, C.-H.; Chang, J.-K. Ionic Liquid Electrolytes with Various Sodium Solutes for Rechargeable Na/$NaFePO_4$ Batteries Operated at Elevated Temperatures. *Appl. Mater. Interfaces* **2014**, *6*, 17564-17570.

(17) Yoon, H.; Zhu, H.; Hervault, A.; Armand, M.; MacFarlane, D. R.; Forsyth, M. Physicochemical Properties of N-propyl-N-methylpyrrolidinium Bis(fluorosulfonyl)imide for Sodium Metal Battery applications. *Phys. Chem. Chem. Phys.* **2014**, *16*, 12350-12355.

(18) Ding, C. S.; Nohira, T.; Hagiwara, R.; Matsumoto, K.; Okamoto, Y.; Fukunaga, A.; Sakai, S.; Nitta, K.; Inazawa, S. Na[FSA]-[C_3C_1pyrr][FSA] Ionic Liquids as Electrolytes for Sodium Secondary Batteries: Effects of Na Ion Concentration and Operation Temperature. *J. Power Sources* **2014,** *269*, 124-128.

(19) Matsumoto, K.; Taniki, R.; Nohira, T.; Hagiwara, R. Inorganic–Organic Hybrid Ionic Liquid Electrolytes for Na Secondary Batteries. *J. Electrochem. Soc.* **2015**, *162*, A1409-A1414.

(20) Forsyth, M.; Yoon, H.; Chen, F.; Zhu, H.; MacFarlane, D. R.; Armand, M.; Howlett, P. C. Novel Na^+ Ion Diffusion Mechanism in Mixed Organic−Inorganic Ionic Liquid Electrolyte Leading to High Na^+ Transference Number and Stable, High Rate Electrochemical Cycling of Sodium Cells. *J. Phys. Chem. C*, in press, (DOI: 10.1021/acs.jpcc.5b11746).

(21) Mandai, T.; Nozawa, R.; Tsuzuki, S.; Yoshida, K.; Ueno, K.; Dokko. K.; Watanabe, M. Criteria for Solvate Ionic Liquids. *J. Phys. Chem. B* **2013**, *117*, 15072-15085.

(22) Matsumoto, H.; Yanagida, M.; Tanimoto, K.; Nomura, M.; Kitagawa, Y.; Miyazaki, Y.; Highly Conductive Room Temperature Molten Salts Based on Small Trimethylalkylammonium Cations and Bis(trifluoromethylsulfonyl)imide. *Chem. Lett.* **2000**, *8*, 922-923.

(23) Matsumoto, K.; Okamoto, Y.; Nohira, T.; Hagiwara, R. Thermal and Transport Properties of $Na[N(SO_2F)_2]$−[*N*-Methyl-*N*-propylpyrrolidinium][$N(SO_2F)_2$] Ionic Liquids for Na Secondary Batteries. *J. Phys, Chem. C* **2015**, *119*, 7648-7655.

(24) Garcia, B.; Lavallee, S.; Perron, G.; Michot, C.; Armand. M. Room Temperature Molten Salts as Lithium Battery Electrolyte. *Electrochim. Acta* **2004**, *49*, 4583-4588.

(25) Ishikawa, M.; Sugimoto, T.; Kikuta, M.; Ishiko, E.; Kono, M. Pure Ionic Liquid Electrolytes Compatible with a Graphitized Carbon Negative Electrode in Rechargeable Lithium-ion Batteries. *J. Power Sources* **2006**, *162*, 658-662.

(26) Matsumoto, H.; Sakaebe, H.; Tatsumi, K.; Kikuta, M.; Ishiko, E.; Kono, M.; Fast Cycling of Li/$LiCoO_2$ Cell with Low-viscosity Ionic Liquids Based on Bis(fluorosulfonyl)imide $[FSI]^-$. *J. Power Sources* **2006**, *160*, 1308-1313.

(27) Matsumoto, H.; Kageyama, H.; Miyazaki, Y.; Effect of Ionic Additives on the Limiting Cathodic Potential of EMI-based Room Temperature Ionic Liquids. *Electrochemistry* **2003**, *71*, 1058-1060.

(28) Matsumoto, H.; Sakaebe, H.; Tatsumi, K. Preparation of Room Temperature Ionic Liquids Based on Aliphatic Onium Cations and Asymmetric Amide Anions and Their Electrochemical Properties as a Lithium Battery Electrolyte. *J. Power Sources* **2005**, *146*, 45-50.

(29) Monti, D.; Jonsson, E.; Palacin, M. R.; Johansson, P. Ionic Liquid Based Electrolytes for Sodium-Ion Batteries: Na^+ Solvation and Ionic Conductivity. *J. Power Sources* **2014,** *245*, 630-636.

(30) Wibowo, R.; Andous, L.; Rogers, E. I.; Jones, S. E. W.; Compton, R. G.; A Study of the Na/Na^+ Redox Couple in Some Room Temperature Ionic Liquids. *J. Phys. Chem. C* **2010**, *114*, 3618-3626.

(31) Matsumoto, K.; Hosokawa, T.; Nohira, T.; Hagiwara, R.; Fukunaga, A.; Numata, K.; Itani, E.; Sakai, S.; Nitta, K.; Inazawa, S. The Na[FSA]-[C_2C_1im][FSA] ($C_2C_1im^+$:1-Ethyl-3-Methylimidazolium and FSA^-:Bis(fluorosulfonyl)amide) Ionic Liquid Electrolytes for Sodium Secondary Batteries. *J. Power Sources* **2014,** *265*, 36-39.

(32) Katayama, Y.; Dan, S.; Miura, T.; Kishi, T. Electrochemical Behavior of Silver in 1-Ethyl-3-methylimidazolium Tetrafluoroborate Molten Salt. *J. Electrochem. Soc.* **2001**, *148*, C102-C105.

(33) Ding, C.; Nohira, T.; Kuroda. K.; Hagiwara, R.; Fukunaga, A.; Sakai, S.; Nitta, K.; Inazawa, S. NaFSA-C_1C_3pyrFSA Ionic Liquids for Sodium Secondary Battery Operating over a Wide Temperature Range. *J. Power Sources* **2013**, *238*, 296-300.

(34) Yamagata, M.; Nishigaki, N.; Nishishita, S.; Matsui, Y.; Sugimoto, T.; Kikuta, T.; Higashizaki, T.; Kono, M.; Ishikawa, M. Charge–discharge Behavior of Graphite Negative Electrodes in Bis(fluorosulfonyl)imide-based Ionic Liquid and Structural Aspects of Their Electrode/electrolyte Interfaces. *Electrochim. Acta* **2013**, *110*, 181-190.

(35) Shkrob, I. A.; Marin, T. W.; Zhu, Y.; Abraham, D. P.; Why Bis(fluorosulfonyl)imide Is a "Magic

Anion" for Electrochemistry. *J. Phys. Chem. C* **2014**, *118*, 19661-19671.

(36) Sugimoto, T.; Kikuta, M.; Ishiko, E.; Kono, M. Ishikawa, M. Ionic Liquid Electrolytes Compatible with Graphitized Carbon Negative without Additive and Their Effects on Interfacial Properties. *J. Power Sources* **2008**, *183*, 436-440.

(37) Piper, D. M.; Evans. T.; Leung, K.; Watkins. T.; Olson, J.; Kim, S. C.; Han, S. S.; Bhat, V.; Oh. K. H.; Buttry. D. A.; Lee. S.-H. Stable Silicon-ionic Liquid Interface for Next-Generation Lithium-ion Batteries. *Natur. Commun.* **2015**, *6*, 6230.